Title: Diffusivities of metal acetylacetonates in liquid ethanol and comparison with the transport behavior in supercritical systems

Authors: Bruno Zêzere, Joana Cordeiro, Jorge Leite, Ana L. Magalhães, Inês Portugal, Carlos M. Silva

PII: S0896-8446(18)30223-7
DOI: https://doi.org/10.1016/j.supflu.2018.06.003
Reference: SUPFLU 4295

To appear in: *J. of Supercritical Fluids*

Received date: 3-4-2018
Revised date: 4-6-2018
Accepted date: 5-6-2018

Please cite this article as: Zêzere B, Cordeiro J, Leite J, Magalhães AL, Portugal I, Silva CM, Diffusivities of metal acetylacetonates in liquid ethanol and comparison with the transport behavior in supercritical systems, *The Journal of Supercritical Fluids* (2018), https://doi.org/10.1016/j.supflu.2018.06.003

Diffusivities of metal acetylacetonates in liquid ethanol and comparison with the transport behavior in supercritical systems

Bruno Zêzere, Joana Cordeiro, Jorge Leite, Ana L. Magalhães, Inês Portugal, Carlos M. Silva*

Department of Chemistry, CICECO, University of Aveiro, 3810-193 Aveiro, Portugal

***Corresponding author.** E-mail: carlos.manuel@ua.pt; tel.: +351 234 401549; fax: +351 234 370084.

GRAPHICAL ABSTRACT

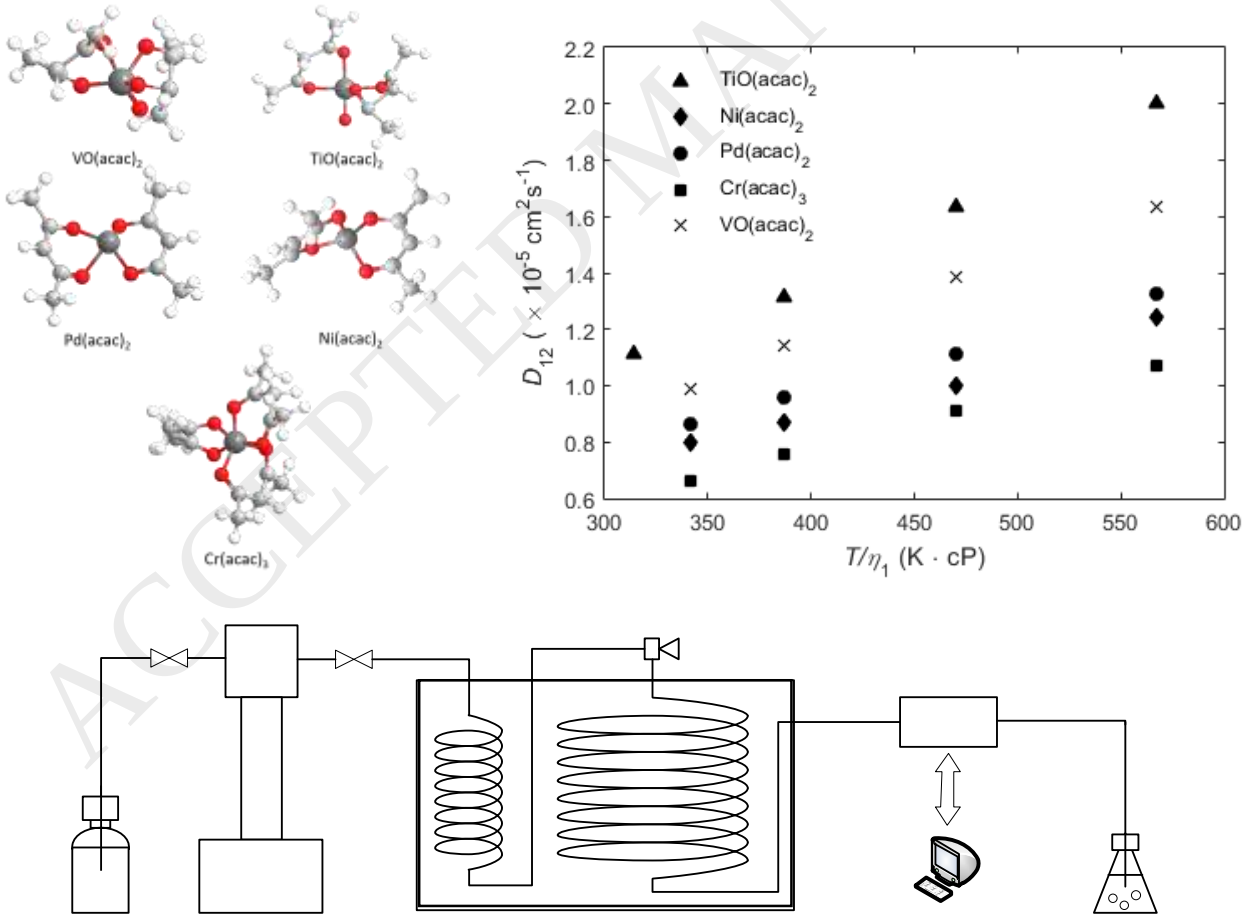

Highlights

- Measurement of diffusivities of five metal acetylacetonates in liquid ethanol
- Solutes: $Pd(acac)_2$, $Cr(acac)_3$, $VO(acac)_2$, $Ni(acac)_2$, and $TiO(acac)_2$,
- Experiments: chromatographic peak broadening method; 1 bar; 303.15-333.15 K
- Comparison of the diffusive behavior in liquid ethanol and in supercritical CO_2
- Nine models adopted. Four of them achieved average errors from 0.55 % to 3.88 %.

Abstract

Diffusion coefficients of chromium(III) acetylacetonate, palladium(II) acetylacetonate, nickel(II) acetylacetonate, vanadyl(II) acetylacetonate, and titanium(IV) oxyacetylacetonate in liquid ethanol were measured by chromatographic peak broadening method (CPB) over the range of temperature 303.15-333.15 K at atmospheric pressure. The dependencies of D_{12} upon temperature and Stokes–Einstein coordinates were examined in detail. Moreover, the experimental data were modelled using nine equations from the literature to test their accuracy and prediction ability. The lower deviations were achieved by the 2-parameter correlation of Dymond-Hildebrand-Batschinski (0.32-2.17 %), the 1-parameter correlation of Tracer Liu-Silva-Macedo (1.58-3.88 %), and the 2-parameter correlations of Magalhães *et al.* (0.55-2.32 %). Finally, the proposed correlation based on hydrodynamic approach was found to well represent palladium(II) acetylacetonate and chromium(III) acetylacetonate systems in

supercritical carbon dioxide and liquid ethanol, with the average absolute relative deviation of 3.15 and 5.02 %, respectively.

Keywords: chromatographic peak broadening method; diffusion coefficient; ethanol; metal acetylacetonate; modeling.

Nomenclature

AARD	Average absolute relative deviation, Eq. (25)
B_{DHB}	Parameter of the solute-solvent interaction in the DHB model
$C(L,t)$	Average concentration of solute at column outlet
CPB	Chromatographic peak broadening
$Cr(acac)_3$	Chromium(III) acetylacetonate
D	Dispersion coefficient
D_{12}	Tracer diffusion coefficient
De	Dean number, $\mathrm{De} = Re\sqrt{\lambda}$
DHB	Dymond-Hildebrand-Batchinski
$k_{12,d}$	Binary interaction constant
k_B	Boltzmann constant
L	Column length

LJ	Lennard-Jones
M	Molecular weight
M_{12}	Reduced molecular weight
m	Mass of a molecule
mSE_1	modified Stokes-Einstein-1
N_{Av}	Avogadro's number
NAI	Normalized absorbance intensity
NDP	Number of data points
$Ni(acac)_2$	Nickel(II) acetylacetonate
p	Number of adjustable parameters of the model
P	Pressure
$Pd(acac)_2$	Palladium(II) acetylacetonate
R	Column inner radius
R^2	Coefficient of determination
R^2_{adj}	Adjusted coefficient of determination
R_c	Column coil radius
Re	Reynolds number
R_g	Universal gas constant
Sc	Schmidt number

SS_{res}	Residual sum of squares
SS_{tot}	Total sum of squares
t	Time
T	Absolute temperature
T_i^*	Reduced temperature using LJ energy component i
$TiO(acac)_2$	Titanium(IV) oxyacetylacetonate
TLSM	Tracer Liu-Silva-Macedo
u_0	Average linear velocity
V	Molar volume
V_{bp}	Molar volume at normal boiling point
V_{D}	Maximum packaging volume of the solvent (DHB model)
$VO(acac)_2$	Vanadyl(II) acetylacetonate
Greek letters	
$\varepsilon_{\mathrm{LJ,i}}$	LJ parameter of component (i = 1, 2) or mixture (i = 12)
ζ	Curvature ratio
η_1	Solvent viscosity
θ_{j}	Merzliak and Pfenning model parameters (j =1 to 5)

λ	Wavelength
ρ_1	Solvent density
$\rho_{n,1}$	Solvent numerical density
σ_i	Molecular diameter of component *i*
$\sigma_{LJ,i}$	Lennard-Jones diameter of component *i*
Subscripts	
1	Solvent
2	Solute
12	Solute-Solvent pair
bp	Property evaluated at normal boiling point
C	Critical property
Superscripts	
*	Reduced quantity
calc	Calculated
exp	Experimental
mix	Mixture

1. Introduction

The knowledge of transport properties, namely diffusivity, viscosity and thermal conductivity, is essential for adequate modeling, design, optimization and scale-up of processes involving mass, heat and momentum transfer phenomena [1]. For instance, processes such as adsorption, ion exchange, membranes, absorption, extraction and heterogeneous reactions are frequently influenced by mass transfer limitations with large impact on equipment sizing.

Diffusion is a spontaneous process by which molecules or ions in solution move driven by chemical potential gradients. In the case of ideal binary mixtures, the diffusive flux of a solute 2 along z direction ($J_{2,z}$) is mathematically described by Fick's first law [2]:

$$J_{2,z} = -C_t D_{12}^{\text{mix}} \frac{dx_2}{dz} \tag{1}$$

where C_t is total molar concentration, x_2 is solute molar fraction, and D_{12}^{mix} is the corresponding binary diffusion coefficient of species 2 through 1 in the mixture. Under limiting dilute conditions ($x_2 \to 0$), D_{12}^{mix} tend to the tracer diffusion coefficient hereafter denoted by D_{12}. The calculation of diffusive fluxes and concentration profiles requires prior knowledge of diffusivity values for each particular system. However, since a reliable universal theory does not exist for both D_{12}^{mix} and D_{12}, due to the complexity of intermolecular potentials involved, the experimental measurement of diffusion coefficients is always necessary.

The empirical mixing rule of Vignes [3] provides a simple tool for the estimation of D_{12}^{mix} in terms of the tracer diffusivity pairs occurring in a multicomponent system. For instance, in the particular case of binary mixtures, both D_{12} and D_{21} are needed together with mole fractions x_1 and x_2:

$$D_{12}^{\text{mix}} = (D_{12})^{x_1}(D_{21})^{x_2} \quad (2)$$

Whenever non-idealities prevail in the mixture, the Maxwell-Stefan approach can be adopted with advantage, which requires the estimation of the well-known thermodynamic factors [4,5].

Taking into account the above-mentioned principles, the relevance of the tracer diffusion coefficients in mass transport calculations emerges naturally. Furthermore, if a solute diffuses through a solvent mixture, it is interesting to possess the accurate tracer diffusivities of that solute in each solvent for estimation purposes. This is especially important in the case of supercritical fluid extraction, where organic cosolvents are frequently introduced as CO_2 modifiers [6–8].

Metal acetylacetonates – generically represented by Me(acac)_n in this work – are organometallic complexes consisting of acetylacetonate anions ($CH_3COCHCOCH_3^-$) and metal cations (M^{n+}), usually of transition metals. These compounds are characterized by high thermal stability and solubility in organic liquids [9–11]. Altogether, these characteristics are exploited in many different industrial applications, being used for example as catalyst in organic reactions such as hydrogenation and epoxydation of olefins [10,11], as additives in the rubber, polymer, plastics and paint industries [12,13], in processes of extraction and separation of metals [14,15], and as semiconductors [16].

In this work, the tracer diffusion coefficients of palladium(II) acetylacetonate, Pd(acac)_2, chromium(III) acetylacetonate, Cr(acac)_3, vanadyl(II) acetylacetonate, VO(acac)_2, nickel(II) acetylacetonate, Ni(acac)_2, and titanium(IV) oxyacetylacetonate, TiO(acac)_2, are measured in pure liquid ethanol and compared with their diffusivities in supercritical CO_2 modified with ethanol. The experimental data is analysed in detail and

modelled using semi-empirical correlations and molecularly based theories. The structural formula of these complexes can be found in Fig. 1.

2. Materials and Methods

2.1. Chemicals

Nickel(II) acetylacetonate, $Ni(acac)_2$, CAS number 3264-82-2, purity of 98 wt.%, was purchased from Acros Organics. The other five acetylacetonates were purchased from Sigma Aldrich: chromium(III) acetylacetonate, $Cr(acac)_3$, CAS number 21679-31-2, purity 99.99 wt.%; palladium(II) acetylacetonate, $Pd(acac)_2$, CAS number 14024-61-4, purity 99 wt.%; vanadyl(II) acetylacetonate, $VO(acac)_2$, CAS number 3153-26-2, purity of 95 wt.%; titanium(IV) oxyacetylacetonate, $TiO(acac)_2$, CAS number 14024-64-7, purity 90 wt.%. Absolute ethanol (CAS number 64-17-5 purity 99.99 wt.%) and carbon dioxide (CAS number 124-38-9, purity 99.999 vol.%,) were bought from Fisher Chemical and Praxair (Portugal) respectively. All chemicals were used directly without further purification.

2.2. Chromatographic Peak Broadening Method

The chromatographic peak broadening method (CPB), also called Taylor's method, is based on the fundamental work formulated by Taylor [17] and later developed and formalized by Aris [18]. The method has been extensively used to measure binary diffusion coefficients, D_{12}, of solutes in pure or mixed solvents [19–30] due to its simplicity and accuracy (average errors around 5 %). The CPB technique is a type of transient response method where an impulse of solute is injected into a laminar flow of solvent and the response is measured at the column outlet. Alizadeh *et al*. [31] provide a

detailed description of the theoretical background. Very briefly, when a small amount of a solute is injected (at $z = 0$) the solute concentration, C, at column outlet (at $z = L$) as a function of time, t, is given by [32]:

$$C(L,t) = \left(\frac{m}{\pi R^2}\right)\frac{1}{2\sqrt{\pi D t}}\exp\left[-\frac{(L-u_0 t)^2}{4Dt}\right] \quad (3)$$

and

$$D \equiv D_{12} + \frac{R^2\, {u_0}^2}{48\, D_{12}} \quad (4)$$

where m is the total mass of injected solute, R is the inner radius of the column, u_0 is the average linear velocity of the solvent, and D is a dispersion coefficient that combines the effects of the parabolic axial profile and the radial molecular diffusion. The tracer diffusion coefficient, D_{12}, can be obtained by fitting the theoretical concentration profile $C^{\mathrm{calc}}(L,t)$ (Eqs. (3) and (4)) to the experimental data, $C^{\mathrm{exp}}(L,t)$, by minimizing the root mean square error, ε [22,32]:

$$\varepsilon(\%) = \left\{\frac{\int_{t_1}^{t_2}\left[C^{\mathrm{exp}}(L,t) - C^{\mathrm{calc}}(L,t)\right]^2}{\int_{t_1}^{t_2}\left[C^{\mathrm{exp}}(L,t)\right]^2}\right\}^{1/2} \times 100 \quad (5)$$

where t_1 and t_2 are distinct times at 10 % peak height of the response curve ($t_2 > t_1$). Funazukuri and co-workers [32,33] established the quality of fitting as acceptable when ε is in the range of 1 to 3 %, and good when ε <1 %.

In order to ensure good results three restrictions should be adhered to: (i) $\mathrm{De}\sqrt{\mathrm{Sc}} < 10$, to neglect the secondary flow effects inside the column [34], where $\mathrm{De} = \mathrm{Re}/\sqrt{\zeta}$ is the Dean number, $\zeta = R_c/R$ is the curvature ratio, R_c is the coil radius, $\mathrm{Re} = 2\rho_1 \bar{u} R/\eta_1$ is the Reynolds number, $\mathrm{Sc} = \eta_1/(D_{12}\rho_1)$ is the Schmidt number, and η_1 and ρ_1 are the solvent viscosity and density, respectively [32,35]; (ii) $D/(u_0\, L) < 0.01$, to guarantee a Gaussian concentration profile resulting from the dispersion of the injected pulse [36];

(iii) $(u_0\, L)/D > 1000$, to ensure negligible perturbations due to temperature or pressure differences between the dispersion column and the detector [37].

2.3. Equipment and procedure

A schematic representation of the experimental apparatus used to measure tracer diffusivities is shown in Fig. 2. A syringe pump (100MD, Teledyne ISCO) was used to feed liquid ethanol to the diffusion column (PEEK tubing with $R = 0.261\times10^{-3}$ m, $L =$ 10.243 m, and $R_c = 0.150$ m) placed inside a controlled temperature oven (LSIS-148 B2V/IC 22, Venticell, MMM Group). The ethanol feed was held at constant temperature and flow rate during a stabilization period (1 – 2 h) to guarantee a steady baseline prior to solute injections. The injected pulses consisted of diluted $\mathrm{Me(acac)_n}$ ethanolic solutions loaded to the solvent stream using an injection valve with a 0.1 μL loop (injector C74H-1674, Valco Instruments Co. Inc.). The outlet solute concentrations were measured using a UV-vis detector (UV Detector 2500, Knauer) set at a previously selected wavelength. For each solute, four to seven pulses were injected, spaced by 10 to 15 min intervals to avoid peak overlapping. The concentrations of the $\mathrm{Me(acac)_n}$ solutions were in the range of 1×10^{-4} to 5×10^{-3} g cm^{-3} to ensure negligible noise in relation to the pulse signal of the studied compounds.

2.4. Setting UV-vis wavelength for optimum D_{12} measurements

The wavelength for UV-vis detection was adjusted for each metal acetylacetonate under study aiming accurate measurements of D_{12}. For this purpose, a wavelength scan was performed to determine the wavelength of maximum absorbance for each $\mathrm{Me(acac)_n}$,

which were globally found to lie between 200-400 nm. Subsequently, several solute injections were performed for each compound and the peaks were recorded at fixed wavelength (λ) within the maximum absorbance range. The D_{12} values were calculated for each λ and the results were analyzed in terms of adjusted error (ε, defined by Eq. (5)).

2.5. Modeling tracer diffusion coefficients

In this work three hydrodynamic models (Eqs. (6)-(8)), one free-volume model (Eq. (9)), two hybrid free-volume models (Eqs. (10)-(21)) and a set of semi-empirical models (Eqs. (22)-(24)) were selected to estimate/correlate tracer diffusivities, D_{12}. The corresponding equations are summarized in Table 1 and briefly presented in this section. The more curious reader is referred to the assigned references.

The Wilke-Chang model [38,39] is a modification of the Stokes-Einstein relation. It is described by Eq. (6), where T is absolute temperature (K), Φ is a dimensionless association factor ($\Phi = 1.5$ for ethanol and 1.0 for carbon dioxide [39]), η_1 is solvent viscosity (cP), M_1 is solvent molecular weight (g mol^{-1}), and $V_{\mathrm{bp},2}$ is the solute molar volume ($\mathrm{cm}^3\ \mathrm{mol}^{-1}$) at its normal boiling point. The Tyn-Calus [39,40] model is a hydrodynamic equation expressed by Eq (7) where $V_{\mathrm{bp},1}$ is the solvent molar volume ($\mathrm{cm}^3\ \mathrm{mol}^{-1}$) at its normal boiling point. Finally, the third hydrodynamic expression is a modified Stokes-Einstein-1 (mSE_1) equation [41] expressed by Eq. (8) where M_2 is the solute molecular weight.

The free-volume model of Dymond–Hildebrand–Batschinski (DHB) [1,42,43] is described by Eq. (9) where V_1 is the molar volume of solvent ($\mathrm{cm}^3\ \mathrm{mol}^{-1}$). The two adjustable parameters are B_{DHB} ($\mathrm{cm}^{-1}\ \mathrm{mol}\ \mathrm{s}^{-1}\ \mathrm{K}^{-1/2}$), a characteristic parameter for

the solute-solvent pair, and V_{D} ($\mathrm{cm^3\ mol^{-1}}$), which is the minimum molar volume necessary for the occurrence of diffusion.

The Tracer Liu-Silva-Macedo (TLSM) model [1,44,45] is a hybrid free-volume model expressed by Eqs. (10)-(19), where M_{12} is the reduced molar mass of the system ($\mathrm{g\ mol^{-1}}$), T_{i}^{*} is the reduced temperature of species i, $\sigma_{\mathrm{eff,i}}$ is the effective hard sphere diameter of species i (cm), $\rho_{\mathrm{n,1}}$ is the number density of the solvent ($\mathrm{cm^{-3}}$), ρ_{l}^{*} is the reduced density of the solvent, $\mathrm{N_{Av}}$ is the Avogadro's number, R_g the ideal gas constant ($8.3144\ \mathrm{J\ mol^{-1}K}$), k_{B} is the Boltzmann constant, $\varepsilon_{\mathrm{LJ,12}}/k_{\mathrm{B}}$ (K) and $\sigma_{\mathrm{LJ,12}}$ (cm) are the Lennard-Jones (LJ) interaction parameters (energy and diameter, respectively) for the solvent/solute pair ($i = 12$). The LJ parameters can be estimated by Eqs. (18)-(19) where $P_{\mathrm{c,i}}$, $T_{\mathrm{c,i}}$ and $V_{\mathrm{c,i}}$ are the critical pressure (bar), temperature (K) and molar volume ($\mathrm{cm^3\ mol^{-1}}$) of species *i*, respectively.

The $\mathrm{TLSM_d}$ correlation [1,44,45] is a modified TLSM model generated by inserting an interaction constant $k_{12,\mathrm{d}}$ into the diameter combining rule of the TLSM model. Hence Eqs. (16) and (17) are replaced by Eqs. (20) and (21).

Magalhães *et al.* [46] published several semi-empirical correlations (e.g., Eqs. (22)-(24)) to express solute diffusivities D_{12} as a function of temperature, solvent viscosity (η_1) and/or density (ρ_1). The parameters a', a'', a''' and b', b'' and b''' are adjustable constants of the models.

The performance of the various models was assessed in terms of average absolute relative deviation (AARD) (Eq. (25)), coefficient of determination (R^2) (Eq. (26)), and, when applicable, the adjusted coefficient of determination (R^2_{adj}) (Eq. (27)).

$$\mathrm{AARD}(\%) = \frac{100}{\mathrm{NDP}} \sum_{\mathrm{i}=1}^{\mathrm{NDP}} \left| \frac{D_{12}^{\mathrm{exp}} - D_{12}^{\mathrm{calc}}}{D_{12}^{\mathrm{exp}}} \right|_{\mathrm{i}} \tag{25}$$

$$R^2 = 1 - \frac{SS_{\mathrm{res}}}{SS_{\mathrm{tot}}} \tag{26}$$

$$R^2_{\mathrm{adj}} = 1 - \left(\frac{\mathrm{NDP}-1}{\mathrm{NDP}-1-p} \right) \frac{SS_{\mathrm{res}}}{SS_{\mathrm{tot}}} \tag{27}$$

where NDP is the number of experimental points, SS_{res} is the residual sum of squares, SS_{tot} is the total sum of squares and p is the number of adjustable parameters of the model [47].

3. Results and discussion

3.1. Validity of the experimental method

The metal acetylacetonates (solids at room temperature) were dissolved in ethanol at concentrations of 5.01×10^{-4}, 4.02×10^{-3}, 1.05×10^{-4}, 4.85×10^{-4} and 3.96×10^{-3} g cm^{-3}, for Ni(acac)$_2$, Pd(acac)$_2$, VO(acac)$_2$ TiO(acac)$_2$, and Cr(acac)$_3$, respectively. These correspond to 1.95×10^{-4}, 1.32×10^{-3}, 3.96×10^{-5}, 1.85×10^{-4}, and 1.13×10^{-3} μmol of solute injected (volume of 0.1 μL) in each assay, respectively. These values are in accordance with data reported in the literature for similar compounds (e.g., phenylbutazone 5.64×10^{-3} μmol [48], chromium(III) acetylacetonate 1.15×10^{-3} μmol [49]), and α-pinene 6.17×10^{-4} μmol [21]), and guarantees the dilute conditions inside the column compatible with tracer diffusivity measurements.

The first step in this work was the selection of the appropriate wavelength (λ) of the UV detector to make the D_{12} measurements for each solute. The preliminary results are presented in Fig. 3 for Ni(acac)$_2$ and VO(acac)$_2$ along with the adjusted error ε (defined by Eq. 5) and the normalized absorbance intensity, defined as NAI $= Abs_{\max}/A_{\text{peak}}$, where $Abs_{\max}$ is the maximum absorbance and A_{peak} is the peak area [50]. It can be seen that D_{12} values fluctuate with the detector wavelength (Fig. 3a). For each Me(acac)_n the best wavelength region was identified so that the D_{12} values had the minimum adjusted error (ε) (Fig. 3b) and best detector linearity accessed by NAI (Fig. 3c). For Ni(acac)$_2$ the best results were obtained in the range from 230 to 250 nm, hence the experimental measurements were made at 236 nm. The same analysis was performed for the other Me(acac)_n, leading to the wavelength selection of 240 nm for Pd(acac)$_2$ and VO(acac)$_2$, 280 nm for TiO(acac)$_2$ and 367 nm for Cr(acac)$_3$.

It is worth mentioning that through this work the CPB method assumptions were always assured, namely: *i*) small linear velocities (< 1.168 cm s^{-1}), and thus laminar flow with Reynolds numbers in the range of 5 – 8; *ii*) longitudinal Peclet numbers ($u_0\, L/D_{12}$) in the order of 10^7, which means axial dispersion can be neglected; *iii*) $\text{De}\sqrt{\text{Sc}} < 10$, indicating the secondary flow effects due to column coiling are negligible; and *iv*) $D/(u_0\, L) < 1 \times 10^{-4}$, demonstrating Gaussian concentration profiles.

3.2. Measured diffusivities of metal acetylacetonates in liquid ethanol

The tracer diffusion coefficients of TiO(acac)$_2$, Ni(acac)$_2$, Pd(acac)$_2$, VO(acac)$_2$ and Cr(acac)$_3$ in ethanol were measured at 1 bar and at fixed temperatures in the range 303.15 to 333.15 K. For each solute, at least 4 injections were made and the D_{12} values were determined by fitting the model (Eqs. (3) – (4)) to the experimental response

curves. The diffusivities listed in Table 2 represent the average of the replicate injections. The density and viscosity of liquid ethanol were taken from Yaws [51] for each experimental condition.

A good agreement was obtained between our results and data available in the literature for $Cr(acac)_3$ in liquid ethanol [52,53], with a deviation of only 1.70 %. For the remaining $Me(acac)_2$ compounds there are no data in the literature for comparison.

The diffusion coefficients for $\mathrm{Me(acac)_n}$ in ethanol are plotted in Fig. 4 as a function of temperature at fixed pressure ($P = 1$ bar). Overall, it can be seen that D_{12} increases almost linearly with temperature, which may be ascribed to the increment of both solvent free volume and solute kinetic energy. In fact, the solute collisions with neighbouring solvent molecules decrease with increasing free volume, which enhances the mean free path of the solute and thus its diffusivity. Furthermore, at higher temperatures the solute molecule possesses higher energy, being able to overcome the activation energy for jumping between adjacent holes or cages in the solvent [1,43].

The dependence of D_{12} on Stokes-Einstein coordinate, T/η_1, is illustrated in Fig. 5. The results evidence a linear relation between the two variables with non-zero intercepts that disclose small deviations from the hydrodynamic behaviour, whose values are 9.891, 0.1672, 2.958, -2.663 and 5.973 (10^{-7} cm^2 s^{-1}) for $Ni(acac)_2$, $Pd(acac)_2$, $VO(acac)_2$, $TiO(acac)_2$, $Cr(acac)_3$, respectively. Similar results have been reported in the literature for other binary systems [19,21,49,54–58] such as for example eucalyptol in ethanol [57], and benzene, phenol, naphthalene and caffeine in SC-CO_2 [56].

The present data reveal that solutes with lower number of acetylacetonate groups exhibit higher binary diffusion coefficients, $D_{12}[Me(acac)_2] > D_{12}$ $[Cr(acac)_3]$, which is related

to their smaller LJ diameters as reported by Cordeiro *et al.* [49], i.e. σ_{LJ} [Me(acac)$_2$] < σ_{LJ} [Cr(acac)$_3$)]. The diffusive behaviour of metal acetylacetonates with two acac groups may be disclosed carrying out molecular dynamics simulations to understand how molecular structure specificities affect D_{12}, where radial distribution functions, spatial distribution functions and coordination numbers may be useful.

3.3. Metal acetylacetonate diffusivity in liquid ethanol and supercritical solvent

Based on hydrodynamic relations it is possible to link D_{12} with system temperature, T, and solvent viscosity, η_1. In Fig. 6, a log-log relation between D_{12}/T and η_1 is observed both in supercritical carbon dioxide (SC-CO$_2$) and in liquid ethanol (EtOH) for Pd(acac)$_2$ and Cr(acac)$_3$ using the data from this work and data reported by Kong *et al.* [52,53] and Cordeiro *et al*. [49]. Once again, it is worth noting the good agreement between literature data and current data, from which a reliable and consistent trend emerges for D_{12} (see Fig. 6, particularly Fig. 6.b).

It is clear from Fig. 6 that the tracer diffusivities are grouped along two distinct segments over the same trend line, one corresponding to the liquid state and the other to the supercritical state. The liquid diffusivities are undoubtedly lower than those in SC-CO$_2$, which was expected in advance due to the higher free volume available for diffusion in the case of SC-CO$_2$, along with the weaker intermolecular forces established between Me(acac)$_n$ and carbon dioxide.

The Magalhães *et al* correlation defined by Eq. (24) [46] is valid for diffusion coefficients of a specific solute in SC-CO$_2$ and/or organic solvents, such as ethanol, reason why it has been selected in this work to represent the $D_{12}/T = f(\eta_1)$ trend. The parameters of adjustment evaluated for each solute are presented in Table 3. The low

AARDs values (3.15 % and 5.02 %) indicate a good correlation of this model for the diffusivity data of $Cr(acac)_3$ and of $Pd(acac)_2$. Noteworthy, this model only requires the solvent viscosity at the studied conditions to evaluate D_{12} values.

3.4. Modelling Results

The various properties required to model the diffusivity data are presented in Table 4, together with their sources and/or estimation methods. The results achieved by the models of Table 1 are listed in Table 5, namely, the fitting parameters (in the case of correlations), relative deviations (AARD, %), coefficients of determination (R^2), and adjusted coefficients of determination (R^2_{adj}). It is possible to observe that AARD values vary significantly, from model to model, and in general the prediction of D_{12} is poor. The DHB model, the $TLSM_d$ model (when applicable) and the Magalhães *et al*. correlations [46] are the ones presenting lower AARD values. Consequently, one may state that these models are the most suitable to estimate the diffusivities of $Me(acac)_n$ in liquid ethanol. Nonetheless it is worth noting that, in the case of $VO(acac)_2$, the predictive hydrodynamic models of Wilke-Chang, Tyn-Calus and mSE1 are all able to calculate diffusivities with very low deviations (3.32 %, 1.03 % and 4.31 %, respectively).

It is once again confirmed that the introduction of an interaction parameter in the diameter combining rule of the TLSM model (see $k_{12,\text{d}}$ in Eq. (20) *versus* Eq. (16)) is sufficient to guarantee the accurate representation of tracer diffusivity data [1,44,45]. In the case of $Pd(acac)_2$ and $Cr(acac)_3$ the average errors drop from 20.31 % and 40.82 % to 1.58 % and 3.88 %, respectively (see Table 5). Furthermore, such low deviations are

well inside the experimental errors usually associated to the chromatographic methods (ca. 5-6 %), and compare very well with those obtained by the 2-parameters equations used in this work (i.e., DHB and Magalhães *et al.*, 0.33-2.17 % and 0.55-2.32 % errors, respectively).

4. Conclusions

Binary diffusion coefficients at infinite dilution (D_{12}) of five metal acetylacetonates ($Ni(acac)_2$, $Pd(acac)_2$, $VO(acac)_2$, $TiO(acac)_2$ and $Cr(acac)_3$) in liquid ethanol were measured by the chromatography peak broadening (CPB) method at fixed temperature (303.15 – 333.15 K) and pressure (1 atm). The D_{12} values presented in this study are consistent with those reported in literature for $Cr(acac)_3$ in liquid ethanol. For the other $Me(acac)_2$ this is the first time D_{12} values are reported. The effect of temperature and solvent viscosity on D_{12} was examined. It was found that D_{12} increases with temperature at a fixed pressure and decreases with viscosity at constant temperature. One of the correlations of Magalhães *et al.* (based on the hydrodynamic approach) was used to represent D_{12} of $Pd(acac)_2$ and $Cr(acac)_3$ in SC-CO_2 and in liquid ethanol. This model represents the data measured over a wide range of conditions from supercritical to liquid states with global deviations of 3.15 % ($Pd(acac)_2$) and 5.02 % ($Cr(acac)_3$). The D_{12} values of the five metal acetylacetonates in ethanol were also correlated with several models being the best results achieved with the $TLSM_d$, the Dymond-Hildebrand-Batschinki and the Magalhães *et al.* correlations (AARD in the range 0.70 – 5.36 %).

Acknowledgements

This work was developed in the scope of the project CICECO-Aveiro Institute of Materials (Ref. FCT UID/CTM/50011/2013), financed by national funds through the FCT/MEC and when applicable co-financed by FEDER under the PT2020 Partnership Agreement.

References

[1] H. Liu, C.M. Silva, Modelling of Transport Properties of Hard Sphere Fluids and Related Systems and its Applications, in: Lect. Notes Phys. 753 Theory Simul. Hard-Sph. Fluids Relat. Syst., Springer, Berlin/Heidelberg, 2008: pp. 37–109.

[2] E.L. Cussler, Diffusion Mass Transfer in Fluid Systems, 3th ed., Cambridge University Press, NY, USA, 1997.

[3] A. Vignes, Diffusion in Binary Solutions. Variation of Diffusion Coefficient with Composition, Ind. Eng. Chem. Fundam. 5 (1966) 189–199.

[4] R. Taylor, R. Krishna, Multicomponent mass transfer, in: Wiley Series in Chemical Engineering, John Wiley & Sons, Inc., New York, 1993.

[5] R. Krishna, J.A. Wesselingh, The Maxwell-Stefan approach to mass transfer, Chem. Eng. Sci. 52 (1997) 861–911.

[6] V.H. Rodrigues, M.M.R. de Melo, I. Portugal, C.M. Silva, Supercritical fluid extraction of Eucalyptus globulus leaves. Experimental and modelling studies of the influence of operating conditions and biomass pretreatment upon yields and kinetics, Sep. Purif. Technol. 191 (2018) 207–213.

[7] M.M.R. de Melo, A. Şen, A.J.D. Silvestre, H. Pereira, C.M. Silva, Experimental and modeling study of supercritical CO2extraction of Quercus cerris cork: Influence of ethanol and particle size on extraction kinetics and selectivity to friedelin, Sep. Purif. Technol. 187 (2017) 34–45.

[8] M.M.R. De Melo, A.J.D. Silvestre, C.M. Silva, Supercritical fluid extraction of vegetable matrices: Applications, trends and future perspectives of a convincing

green technology, J. Supercrit. Fluids. 92 (2014) 115–176.

[9] J.D.B. Smith, Metal acetylacetonates as latent accelerators for anhydride-cured epoxy resins, J. Appl. Polym. Sci. 26 (1981) 979–986.

[10] M.F. Sloan, A.S. Matlack, D.S. Breslow, Soluble catalysts for the hydrogenation of olefins, J. Am. Chem. Soc. 85 (1963) 4014–4018.

[11] N. Indictor, W.F. Brill, Metal Acetylacetonate Catalyzed Epoxidation of Olefins with t-Butyl Hydroperoxide, J. Org. Chem. 30 (1965) 2074–2075.

[12] I.C. McNeill, J.J. Liggat, The effect of metal acetylacetonates on the thermal degradation of poly(methyl methacrylate)—I. Cobalt (III) acetylacetonate, Polym. Degrad. Stab. 29 (1990) 93–108.

[13] W.J. Kroenke, Metal smoke retarders for poly(vinyl chloride), J. Appl. Polym. Sci. 26 (1981) 1167–1190.

[14] J.F. Steinbach, H. Freiser, Acetylacetone in the dual role of solvent and reagent in extration metal chelates, Anal. Chem. 25 (1953) 881–884.

[15] J.P. MacKaveney, H. Freiser, Analytical solvent extraction of vanadium using acetylacetone, Anal. Chem. 30 (1958) 526–529.

[16] T.A. Heimer, S.T. D'Arcangelis, F. Farzad, J.M. Stipkala, G.J. Meyer, An acetylacetonate-based semiconductor−Sensitizer linkage, Inorg. Chem. 35 (1996) 5319–5324.

[17] G. Taylor, Dispersion of Soluble Matter in Solvent Flowing Slowly through a Tube, Proc. R. Soc. A Math. Phys. Eng. Sci. 219 (1953) 186–203.

[18] R. Aris, On the dispersion of a solute in a fluid flowing through a tube, Proc. R. Soc. A Math. Phys. Eng. Sci. 235 (1956) 67–77.

[19] C.M. Silva, E.A. Macedo, Diffusion coefficients of ethers in supercritical carbon dioxide, Ind. Eng. Chem. Res. 37 (1998) 1490–1498.

[20] C.A. Filho, C.M. Silva, M.B. Quadri, E.A. Macedo, Infinite dilution diffusion coefficients of linalool and benzene in supercritical carbon dioxide, J. Chem. Eng. Data. 47 (2002) 1351–1354.

[21] R. V. Vaz, A.L. Magalhães, A.A. Valente, C.M. Silva, Measurement and modeling of tracer diffusivities of alpha-pinene in supercritical CO_2, and analysis of their hydrodynamic and free-volume behaviors, J. Supercrit. Fluids. 107 (2016) 690–698.

[22] T. Funazukuri, C.Y. Kong, S. Kagei, Infinite-Dilution Binary Diffusion Coefficients of 2-Propanone, 2-Butanone, 2-Pentanone, and 3-Pentanone in CO2 by the Taylor Dispersion Technique from 308.15 to 328.15 K in the Pressure Range from 8 to 35 MPa, Int. J. Thermophys. 21 (2000) 1279–1290.

[23] T. Funazukuri, C.Y. Kong, S. Kagei, Binary diffusion coefficients of acetone in carbon dioxide at 308.2 and 313.2 K in the pressure range from 7.9 to 40 MPa, Int. J. Thermophys. 21 (2000) 651–669.

[24] C.M. Silva, C.A. Filho, M.B. Quadri, E.A. Macedo, Binary diffusion coefficients of alpha-pinene and beta-pinene in supercritical carbon dioxide, J. Supercrit. Fluids. 32 (2004) 167–175.

[25] C.A. Filho, C.M. Silva, M.B. Quadri, E.A. Macedo, Tracer diffusion coefficients

of citral and D-limonene in supercritical carbon dioxide, Fluid Phase Equilib. 204 (2003) 65–73.

[26] X. Dong, B. Su, H. Xing, Y. Yang, Q. Ren, Diffusion coefficients of l-menthone and l-carvone in mixtures of carbon dioxide and ethanol, J. Supercrit. Fluids. 55 (2010) 86–95.

[27] O. Suárez-Iglesias, I. Medina, C. Pizarro, J.L. Bueno, Diffusion of benzyl acetate, 2-phenylethyl acetate, 3-phenylpropyl acetate, and dibenzyl ether in mixtures of carbon dioxide and ethanol, Ind. Eng. Chem. Res. 46 (2007) 3810–3819.

[28] I.-H. Lin, C.-S. Tan, Diffusion of benzonitrile in CO_2-expanded ethanol, J. Chem. Eng. Data. 53 (2008) 1886–1891.

[29] C. Pizarro, O. Suárez-Iglesias, I. Medina, J.L. Bueno, Binary diffusion coefficients of 2-ethyltoluene, 3-ethyltoluene, and 4-ethyltoluene in supercritical carbon dioxide, J. Chem. Eng. Data. 54 (2009) 1467–1471.

[30] T. Funazukuri, M. Nishio, Infinite dilution binary diffusion coefficients of C5-monoalcohols in water in the temperature range from 273.2 K to 353.2 K at 0.1 MPa, J. Chem. Eng. Data. 44 (1999) 73–76.

[31] A. Alizadeh, C.A. Nieto de Castro, W.A. Wakeham, The theory of the Taylor dispersion technique for liquid diffusivity measurements, Int. J. Thermophys. 1 (1980) 243–284.

[32] T. Funazukuri, C.Y. Kong, S. Kagei, Impulse response techniques to measure binary diffusion coefficients under supercritical conditions, J. Chromatogr. A. 1037 (2004) 411–429.

[33] C.Y. Kong, T. Funazukuri, S. Kagei, Chromatographic impulse response technique with curve fitting to measure binary diffusion coefficients and retention factors using polymer-coated capillary columns, J. Chromatogr. A. 1035 (2004) 177–193.

[34] J.A. Moulijn, R. Spijker, J.F.M. Kolk, Axial dispersion of gases flowing through coiled columns, J. Chromatogr. A. 142 (1977) 155–166.

[35] T. Funazukuri, C.Y. Kong, S. Kagei, Binary diffusion coefficients in supercritical fluids: Recent progress in measurements and correlations for binary diffusion coefficients, J. Supercrit. Fluids. 38 (2006) 201–210.

[36] O. Levenspiel, W.K. Smith, Notes on the diffusion-type model for the longitudinal mixing of fluids in flow, Chem. Eng. Sci. 50 (1995) 3891–3896.

[37] E.T. van der Laan, Notes on the diffusion-type modeling for longitudinal mixing in flow, Chem. Eng. Sci. 7 (1958) 187–191.

[38] C.R. Wilke, P. Chang, Correlation of diffusion coefficients in dilute solutions, A.I.Ch.E. J. (1955) 264–270.

[39] T.K.S. R.C. REID, J.M. PRAUSNITZ, The properties of gases and liquids, Fifth ed., McGraw-Hill Companies, Inc., New York, 1996.

[40] M.T. Tyn, W.F. Calus, Diffusion coefficients in dilute binary liquid mixtures, J. Chem. Eng. Data. 20 (1975) 106–109.

[41] A.L. Magalhães, R. V. Vaz, R.M.G. Gonçalves, F.A. Da Silva, C.M. Silva, Accurate hydrodynamic models for the prediction of tracer diffusivities in supercritical carbon dioxide, J. Supercrit. Fluids. 83 (2013) 15–27.

[42] J.H. Dymond, Corrected Enskog theory and transport coefficients of liquids, J. Chem. Phys. 60 (1974) 969–973.

[43] J.H. Dymond, E. Bitch, E. Vogel, W.A. Wakeham, V. Vesovic, M.J. Assael, Dense fluids, in: J. Millat, J.H. Dymond, C.A. Nieto de Castro (Eds.), Transp. Prop. Fluids. Their Correl. Predict. Estim., Cambridge University Press, Cambridge, 1996.

[44] H. Liu, C.M. Silva, E.A. Macedo, New Equations for Tracer Diffusion Coefficients of Solutes in Supercritical and Liquid Solvents Based on the Lennard-Jones Fluid Model, Ind. Eng. Chem. Res. 36 (1997) 246–252.

[45] A.L. Magalhães, S.P. Cardoso, B.R. Figueiredo, F.A. Da Silva, C.M. Silva, Revisiting the liu-silva-macedo model for tracer diffusion coefficients of supercritical, liquid, and gaseous systems, Ind. Eng. Chem. Res. 49 (2010) 7697–7700.

[46] A.L. Magalhães, P.F. Lito, F.A. Da Silva, C.M. Silva, Simple and accurate correlations for diffusion coefficients of solutes in liquids and supercritical fluids over wide ranges of temperature and density, J. Supercrit. Fluids. 76 (2013) 94–114.

[47] J.N. Miller, J.C. Miller, Statistics and Chemometrics for Analytical Chemistry Dr Jane Miller completed, 5th ed., Prentice Hall, Gosport, UK, 2005.

[48] C.Y. Kong, K. Watanabe, T. Funazukuri, Diffusion coefficients of phenylbutazone in supercritical CO_2 and in ethanol, J. Chromatogr. A. 1279 (2013) 92–97.

[49] J. Cordeiro, A.L. Magalhães, A.A. Valente, C.M. Silva, Experimental and theoretical analysis of the diffusion behavior of chromium(III) acetylacetonate in supercritical CO2, J. Supercrit. Fluids. 118 (2016) 153–162.

[50] T. Funazukuri, T. Sugihara, K. Yui, T. Ishii, M. Taguchi, Measurement of infinite dilution diffusion coefficients of Vitamin K3 in CO2 expanded methanol, J. Supercrit. Fluids. 108 (2016) 19–25.

[51] C.L. Yaws, Chemical Properties Handbook: Physical, Thermodynamic, Environmental, Transport, Safety, and Health Related Properties for Organic and Inorganic Chemicals, Professional, McGraw-Hill, New York, 1999.

[52] C.Y. Kong, K. Watanabe, T. Funazukuri, Measurement and correlation of the diffusion coefficients of chromium(III) acetylacetonate at infinite dilution in supercritical carbon dioxide and in liquid ethanol, J. Chem. Thermodyn. 105 (2017) 86–93.

[53] C.Y. Kong, Y.Y. Gu, M. Nakamura, T. Funazukuri, S. Kagei, Diffusion coefficients of metal acetylacetonates in supercritical carbon dioxide, Fluid Phase Equilib. 297 (2010) 162–167.

[54] R. V. Vaz, A.L. Magalhães, C.M. Silva, Improved hydrodynamic equations for the accurate prediction of diffusivities in supercritical carbon dioxide, Fluid Phase Equilib. 360 (2013) 401–415.

[55] R. V. Vaz, A.L. Magalhães, C.M. Silva, Prediction of binary diffusion coefficients in supercritical CO2 with improved behavior near the critical point, J. Supercrit. Fluids. 91 (2014) 24–36.

[56] R. Feist, G.M. Schneider, Determination of binary diffusion coefficients of benzene, phenol, naphthalene and caffeine in supercritical CO_2, between 308 and 933 K in the pressure range 80 to 160 bar with supercritical fluid chromatography (SFC), Sep. Sci. Technol. 17 (1982) 261–270.

[57] B. Zêzere, A.L. Magalhães, I. Portugal, C.M. Silva, Diffusion coefficients of eucalyptol at infinite dilution in compressed liquid ethanol and in supercritical CO2/ethanol mixtures, J. Supercrit. Fluids. 133 (2018) 297–308.

[58] J. Leite, A.L. Magalhães, A.A. Valente, C.M. Silva, Measurement and modelling of tracer diffusivities of gallic acid in liquid ethanol and in supercritical CO2modified with ethanol, J. Supercrit. Fluids. 131 (2018) 130–139.

[59] K.M. Klincewicz, R.C. Reid, Estimation of critical properties with group contribution methods, AIChE J. 30 (1984) 137–142.

[60] L. Hangzhou, LookChem,look for chemicals all over the world., Weeqoo Technol. Co. (2008).

[61] M.T. Tyn, W.F. Calus, Estimating liquid molar volume, Processing. 21 (1975) 16–17.

[62] R.C. Reid, J.M. Prausnitz, B.E. Poling, The properties of Gases & Liquids, 5th ed., McGraw-Hill International Editions, New York, 2001.

Figure Captions

Figure 1. Structural formulas of the metal acetylacetonates, $\mathrm{Me(acac)_n}$, studied in this work.

Figure 2. Scheme of the experimental apparatus used to measure tracer diffusion coefficients by CPB technique: 1) liquid ethanol container, 2) syringe pump, 3) pre-heating column, 4) injector, 5) diffusion column, 6) oven, 7) UV-vis detector, and 8) waste container.

Figure 3. Influence of the UV-vis detector wavelength (λ, nm) on the (a) D_{12} measurement, (b) adjusted error ε, and (c) and normalized absorbance (NAI) of $VO(acac)_2$ and $Ni(acac)_2$.

Figure 4. Tracer diffusion coefficients of $\mathrm{Me(acac)_n}$ in liquid ethanol as function of temperature at atmospheric pressure.

Figure 5. Binary diffusion coefficients of $\mathrm{Me(acac)_n}$ in liquid ethanol plotted in Stokes-Einstein coordinates.

Figure 6. Log-log representation of D_{12}/T *versus* solvent viscosity (ethanol and supercritical CO_2) for (a) $Pd(acac)_2$ and (b) $Cr(acac)_3$. Data from this work, Kong *et al.*

[52,53] and Cordeiro *et al.* [49]. The line (Eq. (24)) represents the Magalhães et al correlations [46].

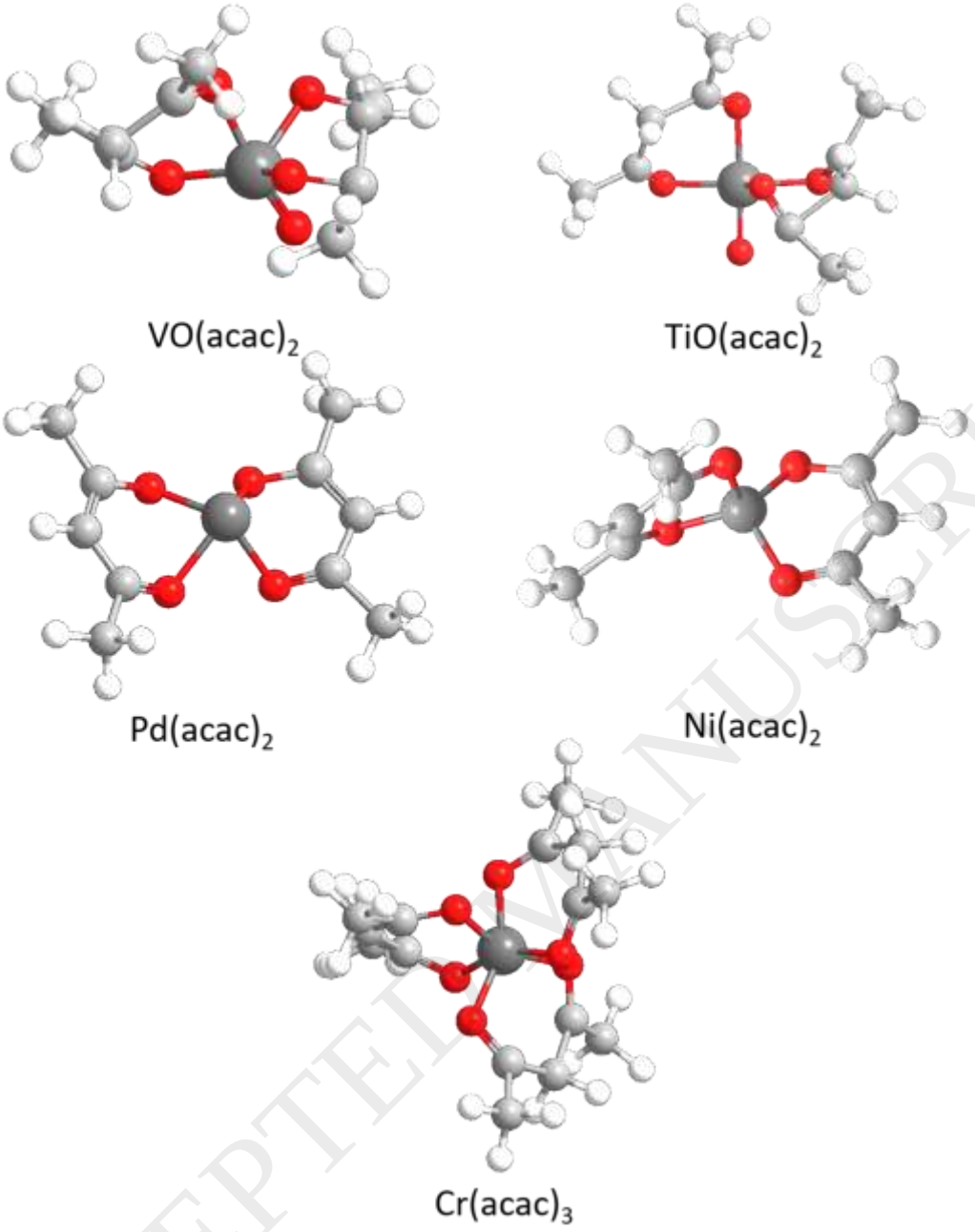

Figure 1. Structural formulas of the metal acetylacetonates, $Me(acac)_n$, studied in this work.

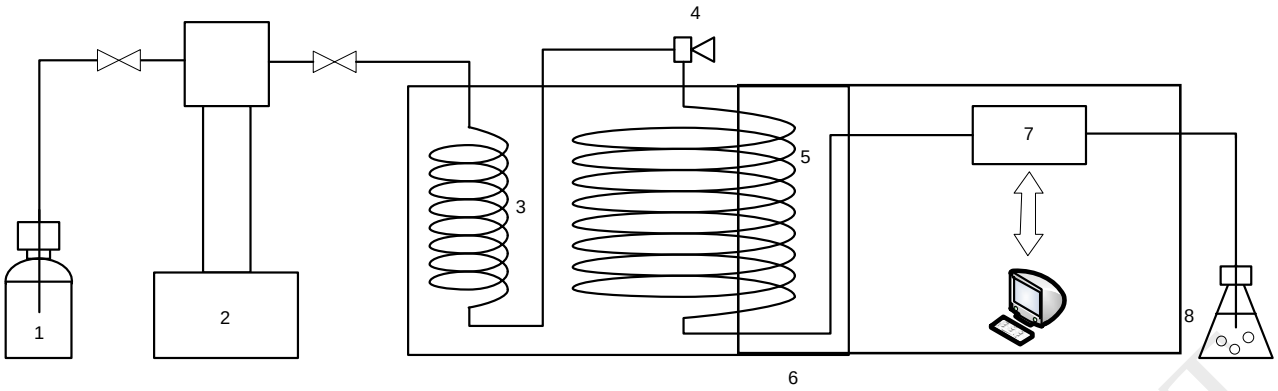

Figure 2. Scheme of the experimental apparatus used to measure tracer diffusion coefficients by CPB technique: 1) liquid ethanol container, 2) syringe pump, 3) pre-heating column, 4) injector, 5) diffusion column, 6) oven, 7) UV-vis detector, and 8) waste container.

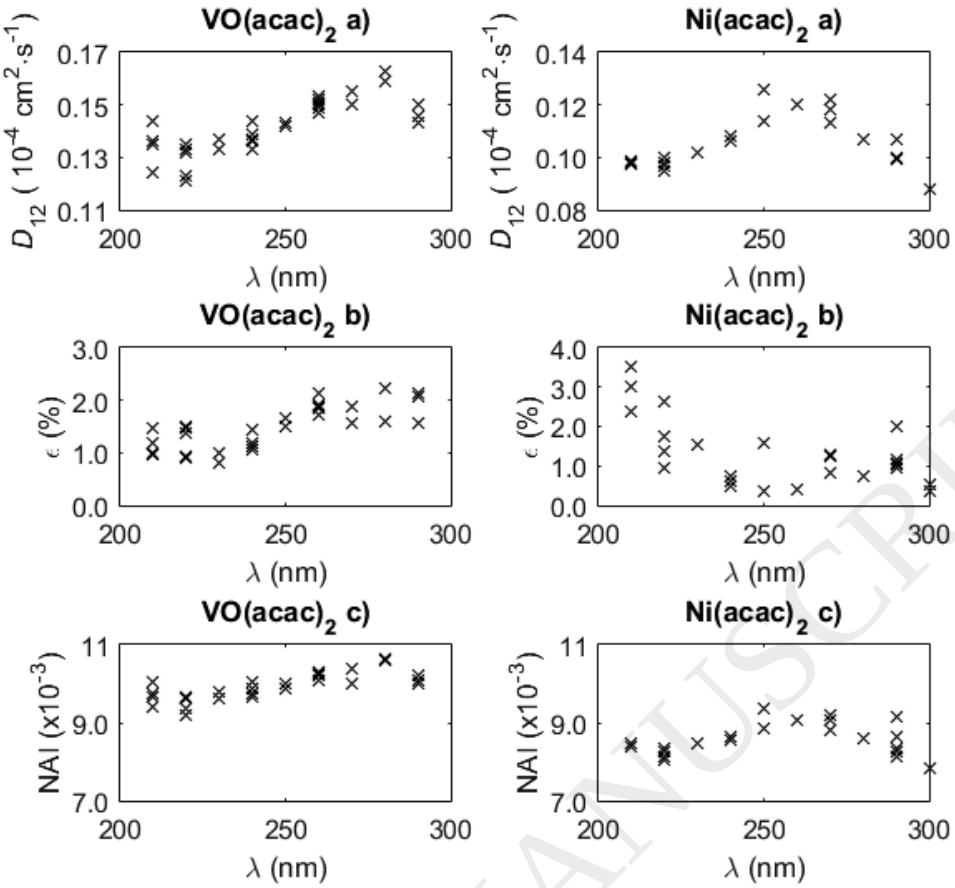

Figure 3. Influence of the UV-vis detector wavelength (λ, nm) on the (a) D_{12} measurement, (b) adjusted error ε, and (c) and normalized absorbance (NAI) of $VO(acac)_2$ and $Ni(acac)_2$.

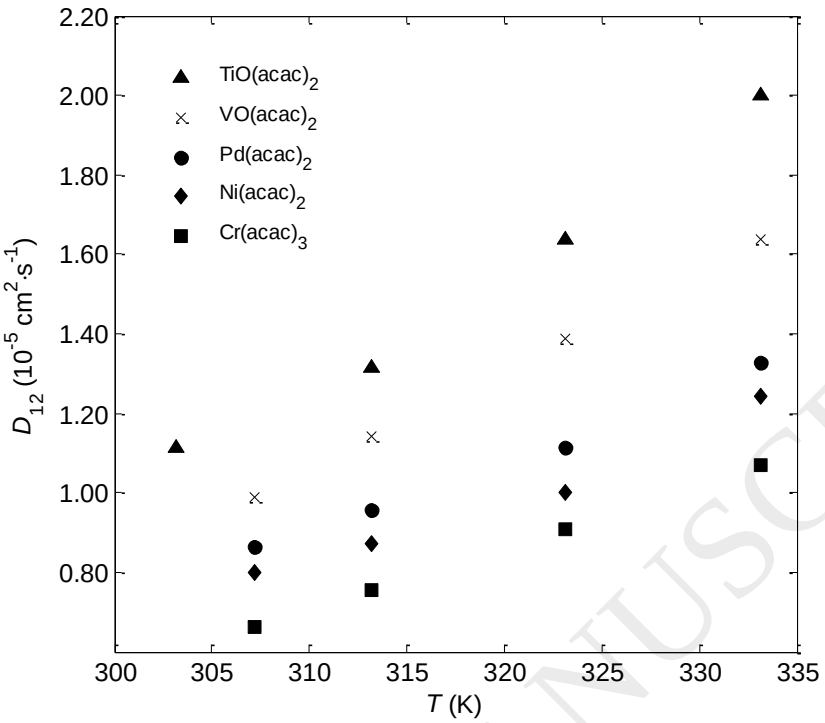

Figure 4. Tracer diffusion coefficients of $Me(acac)_n$ in liquid ethanol as function of temperature at atmospheric pressure.

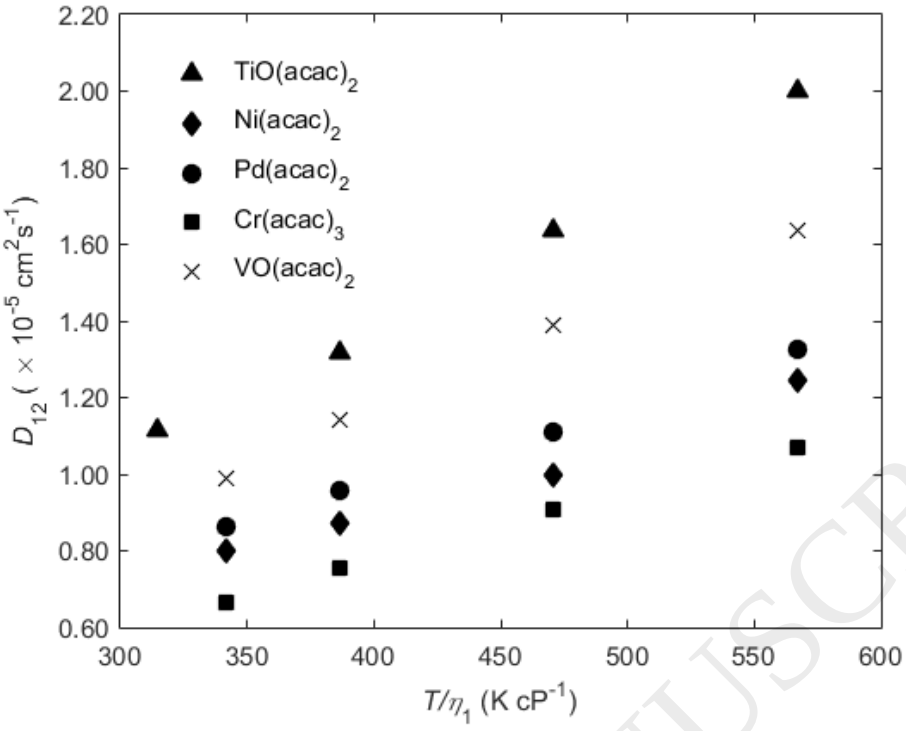

Figure 5. Binary diffusion coefficients of $Me(acac)_n$ in liquid ethanol plotted in Stokes-Einstein coordinates.

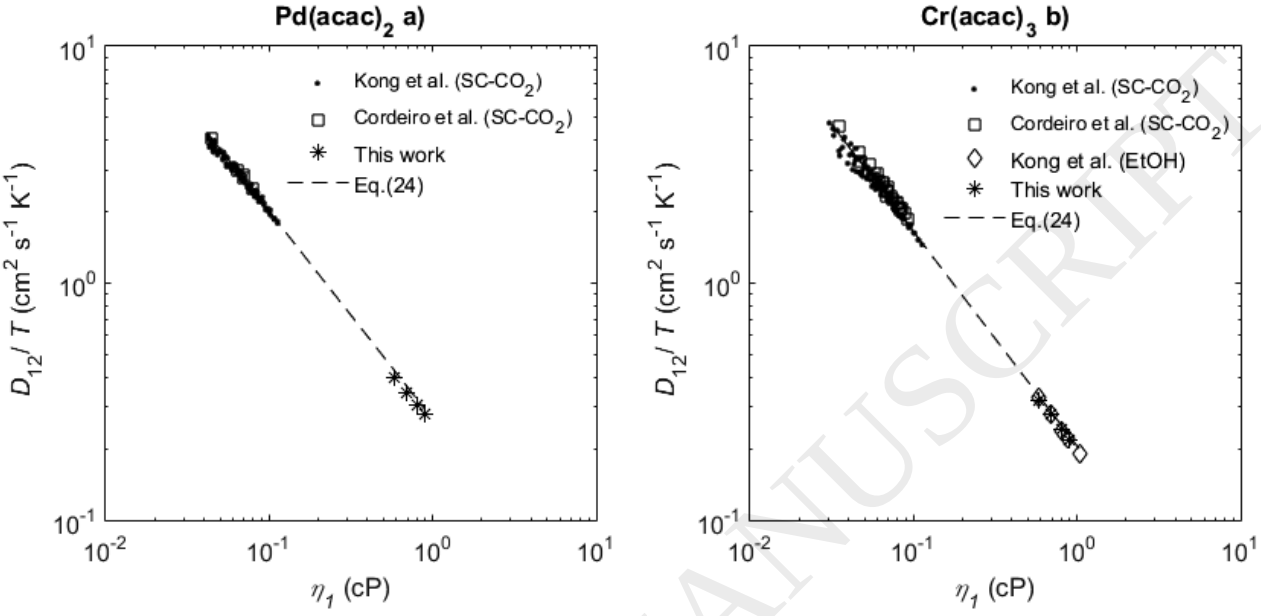

Figure 6. Log-log representation of D_{12}/T *versus* solvent viscosity (ethanol and supercritical CO_2) for (a) $Pd(acac)_2$ and (b) $Cr(acac)_3$. Data from this work, Kong et *al*.

[52,53] and Cordeiro et *al*. [49]. The line (Eq. (24)) represents the Magalhães et al correlations [46].

Tables

Table 1. Models for estimation and correlation of tracer diffusion coefficients ($\boldsymbol{D_{12}}$, $\mathbf{cm^2\ s^{-1}}$).

Wilke-Chang [38,39]	
$D_{12} = 7.4 \times 10^{-8} \frac{T\sqrt{\Phi M_1}}{\eta_1 V_{\mathrm{bp},2}^{0.6}}$	(6)
Tyn-Calus [39,40]	
$D_{12} = 8.93 \times 10^{-8} \frac{V_{\mathrm{bp},1}^{0.267}}{V_{\mathrm{bp},2}^{0.433}} \frac{T}{\eta_1}$	(7)
Modified Stokes-Einstein-1 (mSE$_1$) [41]	
$D_{12} = 1.1335 \times 10^{-6} \left(\frac{T}{\eta_1}\right)^{0.8468} \frac{1}{\left(M_2 1.459 \left(V_{\mathrm{bp},2}\right)^{0.894}\right)^{0.2634}}$	(8)
Dymond–Hildebrand–Batschinski (DHB) [1,42,43]	
$D_{12} = B_{\mathrm{DHB}} \sqrt{T} (V_1 - V_{\mathrm{D}})$	(9)
Tracer Liu-Silva-Macedo (TLSM) [1,44,45]	
$D_{12} = \frac{21.16}{\rho_{\mathrm{n},1} \sigma_{\mathrm{eff},12}^2} \left(\frac{1000 R_{\mathrm{g}} T}{M_{12}}\right)^{1/2} \exp\left(-\frac{0.75\rho_1^*}{1.2588\text{-}\rho_1^*} - \frac{0.27862}{T_{12}^*}\right)$	(10)
$M_{12} = 2\frac{M_1 M_2}{M_1 + M_2}$	(11)
$T_{\mathrm{i}}^* = \frac{T}{\left(\frac{\varepsilon_{\mathrm{LJ,i}}}{k_{\mathrm{B}}}\right)}$, i = 1, 12	(12)
$\sigma_{\mathrm{eff,i}} = \sigma_{\mathrm{LJ,i}} \times 2^{1/6} \left(1 + \sqrt{1.3229 T_{\mathrm{i}}^*}\right)^{-1/6}$, i = 1, 12	(13)

$\rho_1^* = \rho_{n,1}\sigma_{eff,1}^3$	(14)
$\rho_{n,1} = \rho_1 \frac{N_{Av}}{M_1}$	(15)
$\sigma_{LJ,12} = \frac{\sigma_{LJ,1} + \sigma_{LJ,2}}{2}$	(16)
$\frac{\varepsilon_{LJ,12}}{k_B} = \frac{\sqrt{\frac{\varepsilon_{LJ,1}}{k_B}\sigma_{LJ,1}^3 \times \frac{\varepsilon_{LJ,2}}{k_B}\sigma_{LJ,2}^3}}{{\sigma_{LJ,12}}^3}$	(17)
$\frac{\varepsilon_{LJ,i}}{k_B} = 0.774 T_{c,i}$	(18)
$\sigma_{LJ,i}^3(\text{Å}) = 0.17791 + 11.779\frac{T_{c,i}}{P_{c,i}} - 0.049029\left(\frac{T_{c,i}}{P_{c,i}}\right)^2 \quad , \frac{T_{c,i}}{P_{c,i}} \leq 100$	(19.a)
$\sigma_{LJ,i}^3(\text{Å}) = 0.809 V_{c,i}^{1/3} \quad , \frac{T_{c,i}}{P_{c,i}} > 100$	(19.b)
TLSM$_d$ [1,44,45]	
Eqs. (10)-(15), (18) and (19)	
$\sigma_{LJ,12} = \left(1 - k_{12,d}\right)\frac{\sigma_{LJ,1} + \sigma_{LJ,2}}{2}$	(20)
$\frac{\varepsilon_{LJ,12}}{k_B} = 8\frac{\sqrt{\frac{\varepsilon_{LJ,1}}{k_B}\sigma_{LJ,1}^3 \times \frac{\varepsilon_{LJ,2}}{k_B}\sigma_{LJ,2}^3}}{\left(\sigma_{LJ,1} + \sigma_{LJ,2}\right)^3}$	(21)
Magalhães *et al.* [46]	
$\frac{D_{12}}{T} = a'\frac{1}{\eta_1} + b'$	(22)
$\frac{D_{12}}{T} = a''\rho_1 + b''$	(23)
$\ln\left(\frac{D_{12}}{T}\right) = a'''\ln(\eta_1) + b'''$	(24)

Table 2. Experimental tracer diffusion coefficients, D_{12}, of $\mathrm{Me(acac)_n}$ in ethanol, at 1 bar in the range 303.15 to 333.15 K.

Solute	T (K)	${\rho_1}^{(*)}$ (g $\mathrm{cm^{-3}}$)	${\eta_1}^{(*)}$ (cP)	$D_{12} \pm \Delta D_{12}$ ($10^{-5}\mathrm{cm^2\ s^{-1}}$)
$Ni(acac)_2$	307.15	0.779	0.8983	0.789 ± 0.023
	313.15	0.773	0.8100	0.871 ± 0.020
	323.15	0.763	0.6868	1.000 ± 0.023
	333.15	0.753	0.5872	1.244 ± 0.010
$Pd(acac)_2$	307.15	0.779	0.8983	0.865 ± 0.013
	313.15	0.773	0.8100	0.958 ± 0.002
	323.15	0.763	0.6868	1.112 ± 0.003
	333.15	0.753	0.5872	1.328 ± 0.001
$VO(acac)_2$	307.15	0.779	0.8983	0.990 ± 0.025
	313.15	0.773	0.8100	1.141 ± 0.039
	323.15	0.763	0.6868	1.387 ± 0.014
	333.15	0.753	0.5872	1.636 ± 0.012
$TiO(acac)_2$	303.15	0.783	0.9645	1.115 ± 0.035
	313.15	0.773	0.8100	1.315 ± 0.013
	323.15	0.763	0.6868	1.637 ± 0.022
	333.15	0.753	0.5872	2.002 ± 0.035
$Cr(acac)_3$	307.15	0.779	0.8983	0.664 ± 0.006
	313.15	0.773	0.8100	0.756 ± 0.006
	323.15	0.763	0.6868	0.909 ± 0.013
	333.15	0.753	0.5872	1.069 ± 0.005

(*)Taken from Yaws [51].

Table 3. Optimized parameters for Magalhães *et al.* correlation, Eq. (24), and corresponding values of R^2 and AARD.

Solute	a'''	b'''	R^2	**AARD (%)**
$Pd(acac)_2$	-0.8711	-17.440	0.9927	3.15
$Cr(acac)_3$	-0.9044	- 17.701	0.9913	5.02

Table 4. Physical properties of the pure compounds studied in this work.

Compound	CAS	M $g\ mol^{-1}$	T_c K	P_c bar	V_c $mol\ cm^{-3}$	T_{bp} K	V_{bp} $mol\ cm^{-3}$	σ_{LJ} Å	ε_{LJ}/k_B K
$Cr(acac)_3$	21679-31-2	349.92	-	18.9[a]	626.9[a]		243.4[c]	5.7165[d]	845.60[d]
$Ni(acac)_2$	3264-82-2	256.91	-	25.1[a]	431.2[a]	460.8[b]	164.4[c]	-	-
$Pd(acac)_2$	14024-61-4	304.64	-	23.2[a]	435.4[a]	-	166.1[c]	-	-
$VO(acac)_2$	3153-26-2	265.16	-	24.5[a]	445.3[a]	460.8[b]	170.1[c]	6.5514[e]	508.85[e]
$TiO(acac)_2$	14024-64-7	262.08	-	24.6[a]	445.1[a]	-	169.98[c]	-	-
Ethanol	64-17-5	46.07	513.9[f]	61.4[f]	167.1[f]	-	-	4.23748[g]	1291.41[g]
CO_2	124-38-9	44.01	304.1[f]	73.8[f]	93.9[f]	-	-	3.26192[g]	500.71[g]

[a] Estimated by the contribution method of Reid *et al.* [59]; [b] Taken from LookChem [60]; [c] Estimated by the Tyn-Calus method [61]; [d] Taken from Cordeiro *et al.* [49]; [e] Estimated by Eqs. (17)-(19); [f] Taken from Reid *et al.*[62]; [g] Taken from Liu and Silva [1].

Table 5. Modeling results obtained for the experimental diffusivities of $Pd(acac)_2$, $Ni(acac)_2$, $VO(acac)_2$, $TiO(acac)_2$, $Cr(acac)_3$ and in ethanol.

			$Pd(acac)_2$	$Ni(acac)_2$	$VO(acac)_2$	$TiO(acac)_2$	$Cr(acac)_3$
Model	**Equation**						
Wilke-Chang	(6)	AARD (%)	18.03	29.52	3.32	19.09	18.06
Tyn-Calus	(7)	AARD (%)	20.73	32.35	1.03	17.02	28.71
mSE1	(8)	AARD (%)	10.95	27.26	4.31	19.39	34.71
DHB	(9)	AARD (%) / R^2 / R^2_{adj}	1.92/0.9951/0.9927	0.83/0.9771/0.9314	0.55/0.9991/0.9972	2.17/0.9996/0.9988	0.32/0.9997/0.9990
		B_{DHB} (10^{-7}cm^{-1} mol s^{-1} K$^{-1/2}$)	1.1331	1.1574	1.6513	2.0212	1.0307
		V_D (cm^3 mol^{-1})	55.250	54.917	55.704	55.795	55.458
TLSM	(10)-(19)	AARD (%)	20.31	(*)	(*)	(*)	40.82
$TLSM_d$	(10)-(15) + (18)-(21)	AARD (%) / R^2 / R^2_{adj}	1.58/0.9749/0.9245	(*)	(*)	(*)	3.88/0.9499/0.8500
		$k_{12,d}$	−0.10234				−0.19734
Magalhães *et al.*	(22)	AARD (%) / R^2 / R^2_{adj}	0.70/0.9973/0.9919	1.80/0.9840/0.9520	0.79/0.9984/0.9950	1.80/0.9939/0.9817	0.55/0.9991/0.9974
		a' (10^{-5} cm^2 cP s^{-1} K^{-1})	0.77780	0.75853	1.0908	1.3483	1.3483

equations		b' (10^{-6} cm^2 s^{-1} K^{-1})	-0.050449	-0.68273	-2.1322	-3.1325	-3.1325
	(23)	AARD (%) / R^2 / R^2_{adj}	1.20/0.9952/0.9856	2.32/0.9769/0.9308	0.86/0.9954/0.9863	2.16/0.9872/0.9617	0.74/0.9969/0.9906
		a'' (10^{-7} cm^2 cP s^{-1} K^{-1})	-4.7014	-4.6344	-6.8193	-8.0683	-4.2350
		b'' (10^{-7} cm^2 s^{-1} K^{-1})	3.5128	3.8586	5.6316	6.6713	3.5128
	(24)*	AARD (%) / R^2 / R^2_{adj}	-	1.66/0.9793/0.9378	1.01/0.9960/0.9879	1.41/0.9924/0.9771	-
		a''' (cm^2 cP s^{-1} K^{-1})	-	-0.85724	-0.98533	-1.0020	
		b''' (cm^2 s^{-1} K^{-1})		-17.580	-17.345	-17.1717	

(*) The models were not applied since reliable predictive models or critical constants of the solutes were not found in the literature.